Hydrodynamic Characteristics and Adsorption Particularity of Nanobiological Feedstock Along the Bed Height in a Novel Chromatography Column

Mohsen Jahanshahi, Mohammad Taghi Hamed Mosavian & Elham Sadat Taheri Otaghsara

Chromatographia
An International Journal for Rapid Communication in Chromatography, Electrophoresis and Associated Techniques

ISSN 0009-5893

Chromatographia
DOI 10.1007/s10337-012-2235-3

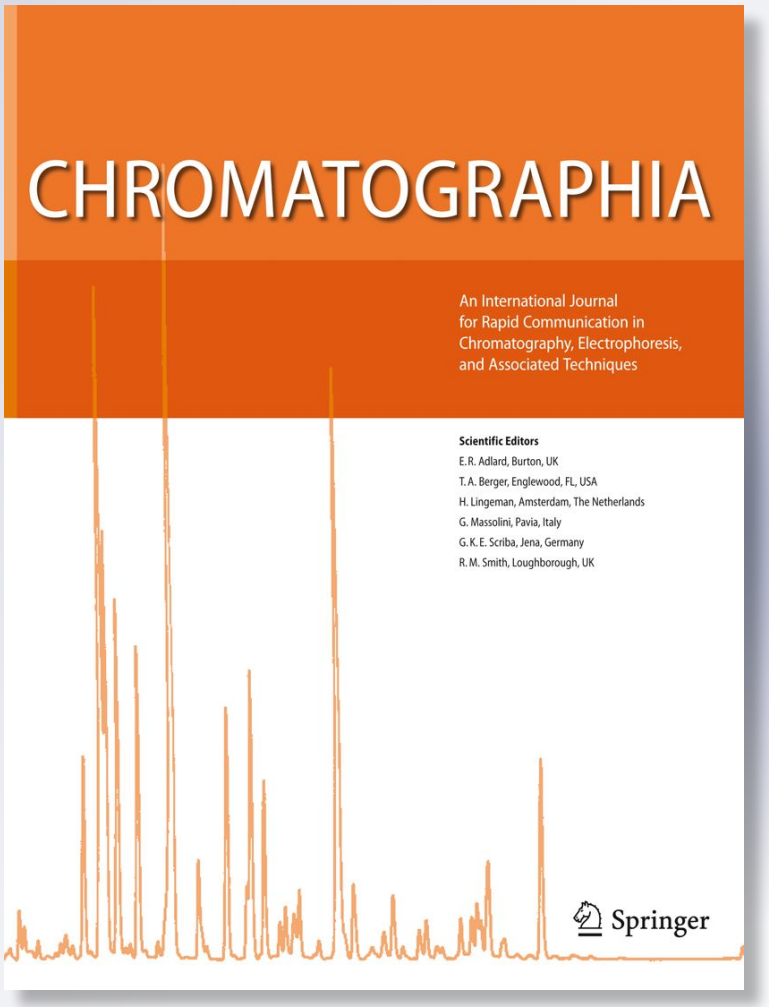

Springer

Chromatographia
DOI 10.1007/s10337-012-2235-3

ORIGINAL

Hydrodynamic Characteristics and Adsorption Particularity of Nanobiological Feedstock Along the Bed Height in a Novel Chromatography Column

Mohsen Jahanshahi · Mohammad Taghi Hamed Mosavian · Elham Sadat Taheri Otaghsara

Received: 17 November 2011 / Revised: 16 March 2012 / Accepted: 22 March 2012

Abstract Expanded bed adsorption (EBA) is a practical method for the separation of nanoparticulates. In order to analysis the local hydrodynamic and adsorption behavior of nanoparticle (NP)-based biological feedstock, a modified Nano Biotechnology Group EBA column with a 26-mm inner diameter was used to withdraw liquid from different axial positions of the column. Fabricated egg albumin (EA) NPs with an average size of 70 nm were employed as a model system and viral size/charge mimic to assess the relationship between hydrodynamic and adsorption performance of NPs at the different column regions. The effects of influential factors, including flow velocity and initial concentration of NPs, on NP hydrodynamic behavior and adsorption kinetics along the bed height were investigated. NP hydrodynamic studies confirmed that non-uniform behavior dominated the system and a decreasing trend of liquid mixing/dispersion with increase of bed height was observed in this column. The results demonstrated an increase in the mixing/dispersion at certain bed heights with the increase in both the velocity and feed initial concentration. Breakthrough curves were measured at various column points to determine the adsorption performance [dynamic binding capacity (DBC) and yield] in different bed positions/zones. Yield and DBC of NPs were improved along the bed height, whereas liquid velocity had the opposite effect. Increasing the initial concentration of NPs enhanced only the DBC. Separation of EA NPs under optimal conditions was 87 %, which is an excellent result for a one-pass frontal chromatography method.

Keywords EBA chromatography · Modified NBG column · EA NPs · Axial hydrodynamic behavior · Axial adsorption performance

List of symbols

B_o	Bodenstein number
C	Exit concentration of NPs in bed effluent (kg m^{-3})
C_o	Initial concentration of NPs (kg m^{-3})
C_9	Exit concentration that has left the 9-cm sample port and is measured at this port (kg m^{-3})
C_{12}	Exit concentration that has left the 12-cm sample port and is measured at this port (kg m^{-3})
D_{axl}	Axial dispersion coefficient (m^2 s^{-1})
H	Bed height (m)
H_{sb}	Settled bed height (m)
h	Axial bed height (m)
N	Theoretical plate
$\bar{t}$	Residence time (s)
U	Superficial flow velocity (m s^{-1})
$V_{f,9}$	Volume of feed loaded onto the column until C_9 reaches a certain degree of NP breakthrough (m^3)
$V_{f,12}$	Volume of feed loaded onto the column until C_{12} reaches a certain degree of NP breakthrough (m^3)
V_l	Liquid volume above the particles in the sampling syringe (m^3)
$V_{L,0-9}$	Liquid volume present in the bed voidage for the 0- to 9-cm column zone (m^3)

M. Jahanshahi (✉) · E. S. T. Otaghsara
Nanotechnology Research Institute, Faculty of Chemical Engineering, Babol University of Technology, P.O. Box 484, Babol, Iran
e-mail: mmohse@yahoo.com; Mjahan@nit.ac.ir
URL: http://nano.nit.ac.ir/IndexEn.aspx

M. T. H. Mosavian
Faculty of Chemical Engineering,
Ferdowsi University of Mashhad, Mashhad, Iran

Published online: 13 April 2012

$V_{L,0-12}$ Liquid volume present in the bed voidage for the 0- to 12-cm column zone (m^3)
$V_{s,0-9}$ Settled volume of adsorbent in the 0- to 9-cm column zone (m^3)
$V_{s,9-12}$ Settled volume of adsorbent in the 9- to 12-cm column zone (m^3)
V_o Volume of the particles in the sampling syringe (m^3)

Greek letters

ε Bed voidage
ε_i Local bed voidage at *i*th layer of bed
δ Variance (s)

Introduction

Economic pressure on the biotechnology downstream processes for producing biological, pharmaceutical, and diagnostic products has recently increased. Many biological products are nanoparticulate in nature and have complex biological structures composed of one or more types of proteins, lipids, and/or nucleic acids. Attention has focused on the applications of such nanoparticles (NPs), e.g., protein NPs as drug delivery vehicles, plasmid DNA and viruses as gene therapy vectors, and virus-like particles as vaccine components. Given this diversity in NPs, there are clearly greatly different operational problems in their recovery and purification [1, 2].

Expanded bed adsorption (EBA) chromatography is a promising bioseparation technique that has been employed to capture nano/bioproducts directly from unclarified suspensions in liquids, e.g., fermentation broths and cell homogenates, without the risk of blocking. The EBA method is able to integrate primary purification, concentration, centrifugation, microfiltration, and other clarification prior steps into a single processing unit. Having these advantages, makes it possible to ensure high process efficiency, decrease the operation time, reduce the final costs of the product, and enhance the product quality [3–9]. It is desirable to know detailed information on the hydrodynamic characteristics and adsorption performance of nano/bioproducts in the EBA system to achieve better design, tighter control, scale-up, optimization, and finally greater efficiency of the EBA operation [10–13]. Compared with classical packed bed and fluidized bed operations, the EBA process has unique properties and acts in ways that combine features of both traditional packed bed and fluidized bed chromatography. The development of special adsorbents with suitable (relatively high) density and wide particle size distribution properties is challenging; these adsorbents cause the formation of a stable classified bed with low back-mixing through the column [6–8, 13, 14]. Non-uniform distribution of particle size, bed voidage, and liquid mixing/dispersion along the bed axis are established in the EBA system. Large and dense particles are located close to the base of the column, while smaller particles with lower density are present towards the top. This classification of adsorbent in the column is accompanied by an increase of bed voidage with the bed height. Researchers have confirmed that notably less mixing and dispersion occur in the zones near the top of bed but they appear to be most intense in the bottom of bed [10, 15–19]. Distribution of these hydrodynamic characteristics as well as the nature of the target component and ligand coupled to the solid matrix could have a significant impact on the nano/bioproducts adsorption particularity including breakthrough curve (BTC) trend, dynamic binding capacity (DBC), and process efficiency within the EBA system. Moreover, experimental and mathematical studies in the literature have proved that the adsorption behavior of bioproducts in the EBA column is non-uniform, and that DBC and BTC trend vary at different locations of the bed [11, 12, 18]. Generally, the design of the column configuration is another critical effective factor in the formation of excellent hydrodynamic properties. Recently, a simple customized Nano Biotechnology Group (NBG) EBA column was constructed by our group (Babol University of Technology) and was employed successfully for recovery and purification of nano/bioproducts [1, 2, 20, 21]. In our previous work, an ordinary NBG column was modified to examine axial changes of clean feedstock (buffer) hydrodynamic parameters within this new design contactor (unpublished data).

In this work, we evaluated the axial hydrodynamics of real nanobiological feedstock to find correct basic relationships between hydrodynamic and adsorption behavior of nanobioproducts in an EBA process. Fabricated egg albumin (EA) NPs were employed as feedstock in this research. Residence time distribution (RTD) analysis was performed at the different points of the modified NBG column to provide information about the axial variation of NP feedstock hydrodynamic performance. In addition, NP breakthrough experiments were carried out in the modified NBG column. BTCs were determined at various bed positions and the DBC and yield as adsorption parameters were calculated. In addition, the effect of two operational variables—fluid velocity and initial concentration of NPs—on the hydrodynamic and adsorption properties of the NPs was studied.

Materials and Methods

Materials

Streamline DEAE adsorbent was purchased from Amersham Bioscience (Uppsala, Sweden). Particle size distribution was in the range of 100–300 μm, mean particle size

was 200 μm, and particle density was approximately 1,200 kg m^{-3}.

EA (very high purity) and glutaraldehyde (25 % solution) were commercially supplied by Sigma Aldrich. Acetone and NaCl were prepared from Merck (Germany).

Modified EBA Contactor and Sampling Device

A modified NBG expanded bed glass column was employed in these studies. The ordinary NBG column was a simple customized device built by our group (Babol University of Technology). The contactor was equipped with a simple sintered glass distributor comprising a 100-μm mesh. The column had a 26-mm inner diameter, 30-cm height, and was divided into nine zones by eight 2- to 2.5-mm sampling holes located every 3 cm along the bed height. A net adapter was placed at the top of the column and was lowered to 0.5 ± 0.2 cm above the bed surface to minimize the dead volume of the system during the experiments. Sampling holes were sealed well enough by moveable rubber bands before experiments were carried out. In order to perform RTD analysis and BTC determination, a metal needle with an inner diameter less than 0.1 mm was used to withdraw only liquid from each sampling hole. Figure 1 shows a schematic of the modified NBG column and equipment configuration used for EBA experiments in this study.

Preparation of NP Feedstock

EA is an attractive protein with favorable physicochemical properties and important features. Preparation of EA NPs in the unique range was performed by a simple coacervation method. Studies by our team on other proteins such as gelatin, human serum albumin (HSA), bovine serum albumin (BSA), and α-lactalbumin have established that this method is good and suitable to prepare protein NPs [22–26]. Thus, 20 mg mL^{-1} of aqueous solution of EA at pH 7 and 35 °C was stirred at 600 rpm by a magnetic stirrer and then 1 mL acetone (desolvating agent) was added dropwise until the solution become just turbid. After the desolvation process, 300 μL of 25 % glutaraldehyde was added as a cross-linking agent and stirred at room temperature for 12 h. The NP sample was purified with 4,000 rpm centrifuge for 20 min after which the supernatant was dialyzed.

The size distribution and mean particle size of the fabricated NPs were analyzed by photon correlation spectroscopy (PCS) and the results are shown in Fig. 2c. The mean particle size of the prepared EA NPs obtained was 70 nm; however, NPs with a diameter of less than 70 nm were also observed. Atomic force microscopy (AFM) was also employed for analysis of the NP morphology and surface information, and the results are shown in Fig. 2a, b. As can be seen from Fig. 2a, b, the desired shape and surface characteristics were achieved successfully, i.e., the NPs were semispherical and had smooth surfaces.

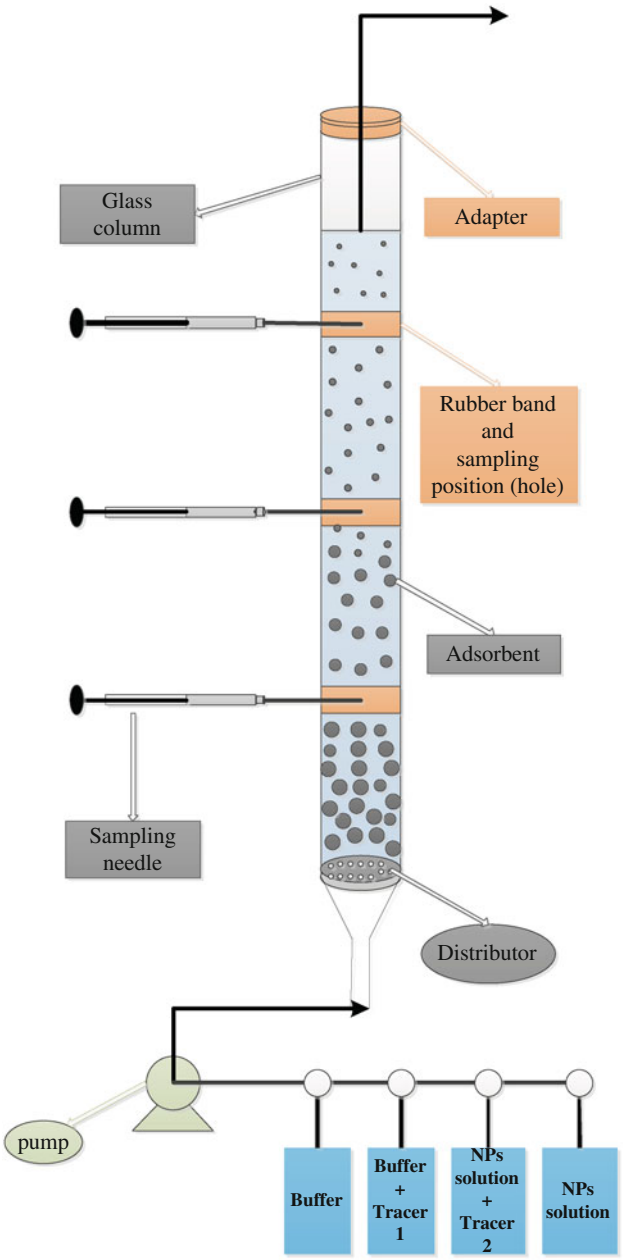

Fig. 1 Schematic of modified NBG column and EBA system setup

Determination of Hydrodynamic Characteristics

Measurement of Local Bed Voidage (ε)

A direct sampling method was carried out to estimate local bed voidage along the bed height [17]. The column with a settled bed height (H_{sb}) of 6 ± 0.1 cm was packed with the

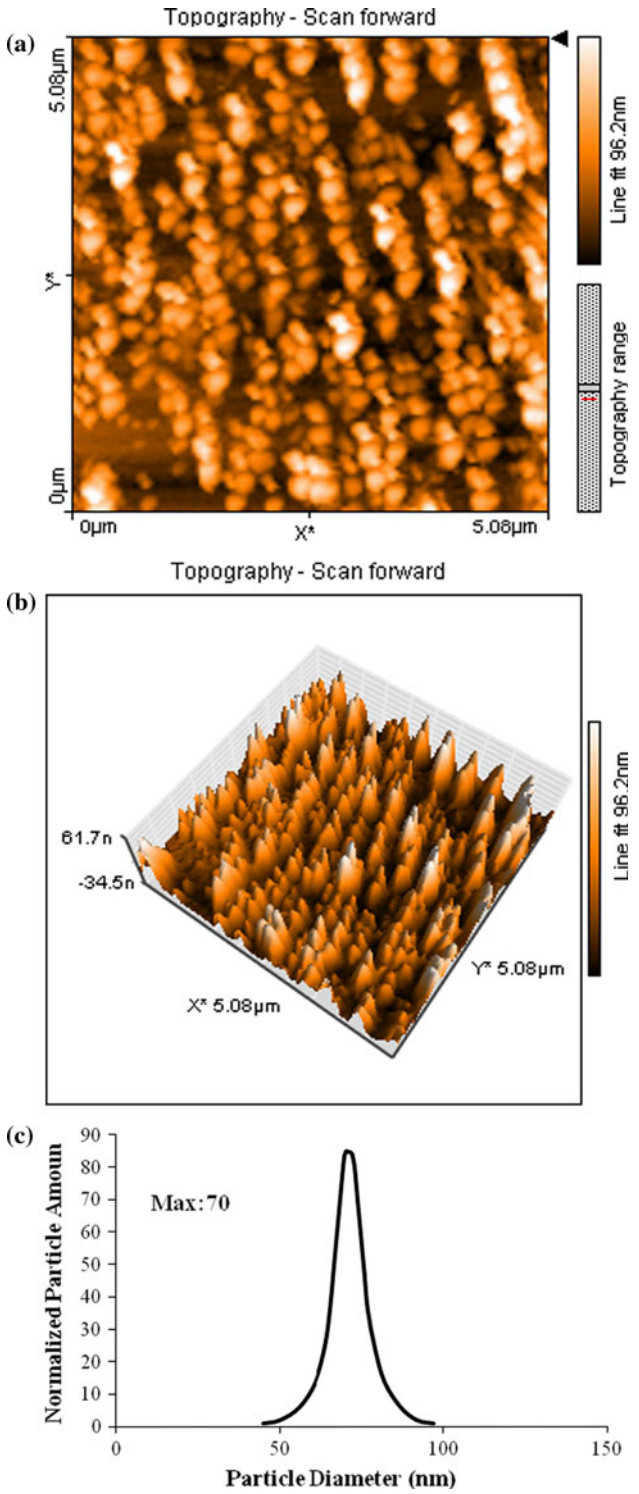

Fig. 2 PCS and AFM analyses of EA NPs: **a** 2D AFM image, **b** 3D AFM image, **c** PCS analysis (size distribution and mean particle size of fabricated EA NPs)

adsorbent and expanded to a stable height for 45–60 min in the distilled water buffer. A metal sampling needle with a 1.5-mm inner diameter connected to a 1-mL graduated syringe was used for this experiment. The needle was inserted into the column center through each sampling hole for 30 min, then adsorbent particles and liquid (1 mL) were simultaneously withdrawn (in less than 3 s). After that, the sample was withdrawn, the needle was taken out, and the sampling hole was sealed with rubber. The syringe was placed vertically (about 2.5–3 h) until particles were settled perfectly. The volumes of the particles that settled in the syringe and the liquid above the particles were obtained. The voidage was determined by Eq. 1

$$\varepsilon_i = \frac{0.4V_o + V_1}{V_o + V_1} \quad (1)$$

where ε_i is the local bed voidage at the ith layer of the bed, V_o is the volume of the particles in the sampling syringe, and V_1 is the liquid volume above the particles.

After these steps, samples were returned into the column and bed was re-expanded for measurement of voidage in other sampling positions. This experiment was carried out at each of the sample ports along the bed one by one and repeated three times at each position. The experimental conditions are illustrated in Table 1.

Measurement of RTD, Bodenstein Number (B_o), and Axial Dispersion Coefficient (D_{axl})

RTD analyses in the various positions along the bed height were performed by using a negative step signal method in order to determine liquid mixing and dispersion within the column [27–29]. Experiments were carried out with the adsorbent to a settled bed height of 6 ± 0.1 cm. Two different types of tracers were employed: (1) a dilute acetone [1 % (v/v)] for buffer feedstock and (2) NaCl solution (20 mM) for NP feedstock.

Acetone was used as the input to the column in the blank systems expanded with suitable buffer (distilled water) alone and tracer concentrations in each sampling position of the bed were measured spectrophotometrically at 280 nm. In contrast, in order to measure the NP feedstock RTD, after stable expansion of the bed with distilled water, a solution of NPs containing NaCl (20 mM) was introduced into the column; this solution was abruptly switched to a solution of NPs alone to achieve a negative step change in ionic strength and tracer conductivity in the sampling effluent that were registered by a conductivity meter. Sampling methods were performed in the center of the column and repeated in each of the bed sampling points one by one. Experiments were repeated in triplicate at each point to ensure consistency. The experimental conditions are summarized in Table 1. RTD measurements in each position were used to estimate Bodenstein numbers and axial dispersion coefficients in expanded bed operation.

Table 1 Conditions for all experiments in this study

Conditions for hydrodynamic experiments in the EBA system			
Clean feedstock		NP feedstock	
Voidage experiment	RTD experiment	RTD experiment	
	Tracer: acetone 1 % (v/v)	Tracer: NaCl (20 mM)	
$U_1 = 4.2 \times 10^{-4}$ m s^{-1}	$U_1 = 4.2 \times 10^{-4}$ m s^{-1}	$U_1 = 4.2 \times 10^{-4}$ m s^{-1}	$C_{o1} = 250$ ppm
$H/H_{sb} = 1.88$	$H/H_{sb} = 1.88$	$C_{o2} = 500$ ppm	$U_2 = 6.3 \times 10^{-4}$ m s^{-1}
$U_2 = 6.3 \times 10^{-4}$ m s^{-1}	$U_2 = 6.3 \times 10^{-4}$ m s^{-1}	$U_2 = 6.3 \times 10^{-4}$ m s^{-1}	$C_{o2} = 500$ ppm
$H/H_{sb} = 2.17$	H/H_{sb}v2.17	$C_{o2} = 500$ ppm	$U_2 = 6.3 \times 10^{-4}$ m s^{-1}
$U_3 = 8.15 \times 10^{-4}$ m s^{-1}	$U_3 = 8.15 \times 10^{-4}$ m s^{-1}	$U_3 = 8.15 \times 10^{-4}$ m s^{-1}	$C_{o3} = 750$ ppm
$H/H_{sb} = 2.5$	$H/H_{sb} = 2.5$	$C_{o2} = 500$ ppm	$U_2 = 6.3 \times 10^{-4}$ m s^{-1}
Conditions for adsorption experiments in the EBA system			
$C_{o1} = 250$ ppm	$U_1 = 4.2 \times 10^{-4}$ m s^{-1}	$U_1 = 6.3 \times 10^{-4}$ m s^{-1}	$C_{o1} = 250$ ppm
	$U_2 = 6.3 \times 10^{-4}$ m s^{-1}		$C_{o2} = 500$ ppm
	$U_3 = 8.15 \times 10^{-4}$ m s^{-1}		$C_{o3} = 750$ ppm

These parameters were obtained by two and three correlations [29–31].

$$B_o = 2N = 2\frac{\overline{t^2}}{\delta^2} \tag{2}$$

$$D_{axl} = \frac{UH}{B_o \varepsilon} \tag{3}$$

where $\bar{t}$ and δ are the residence time and variance, U is the superficial flow velocity, H is the bed height, and N is the number of theoretical plates.

EBA Operation

Measurement of BTCs

The breakthrough analyses were carried out with a settled bed height of 6 ± 0.1 cm. Prior to application of the solution of NPs , the bed was first allowed to reach the stable expansion condition in distilled water buffer. Subsequently unclarified feedstock containing NPs was loaded onto the bed and routinely continued until values of C/C_o approached or equaled 1.0. In order to perform the BTC measurement, the tip of the sample needle was inserted into the column center and the exit concentration of NPs at certain sampling points was recorded spectrophotometrically at 280 nm. The conditions used in this experiment are presented in Table 1. Experiments were repeated three times at each position to ensure consistency.

Estimation of Adsorption Characteristics (DBC and Yield %)

The BTCs obtained at the different column positions were used to calculate the DBC and yield (%).

DBC is usually defined as the amount of NPs adsorbed per volume of adsorbent when the NP exit concentration in the bed effluent attains a certain fraction of the load concentration [18, 32].

DBC at a particular bed position (e.g., $h = 9$ cm) can be represented as follows:

$$\mathrm{DBC}_{9cm} = \frac{C_o V_{f,9} - C_o V_{L,0-9} - \int_0^{V_{f,9}} C_9 \, dV}{V_{s\,0-9}} \tag{4}$$

where C_o is the initial concentration of NPs fed onto the bed, C_9 is the exit concentration that has left the 9-cm sample port and is measured at this port, $V_{f,9}$ is the volume of feed loaded onto the column until C_9 reaches a certain degree of NP breakthrough, $V_{L,0-9}$ is the liquid volume present in the bed voidage for the 0- to 9-cm column zone, and $V_{s,0-9}$ is the settled volume of adsorbent in the 0- to 9-cm column zone. The bed voidage data reported in Table 2 were employed to estimate the relevant adsorbent volume for the DBC calculation.

The DBC for a bed region of interest (e.g., 9–12 cm) at the predetermined extent of NP breakthrough was described by the amount of NPs bound between the 9- and 12-cm ports divided by the adsorbent volume present in this region as follows:

$$\mathrm{DBC}_{9-12} = \frac{\left[C_o V_{f,12} - C_o V_{L,0-12} - \int_0^{V_{f,12}} C_{12} \, dV\right] - \left[C_o V_{f,12} - C_o V_{L,0-9} - \int_0^{V_{t,12}} C_9 \, dV\right]}{V_{s,9-12}} \tag{5}$$

Table 2 Variation of hydrodynamic parameters at various column positions or zones under different liquid superficial velocities (clean feedstock)

Different sampling positions	$U_1 = 4.2 \times 10^{-4}$ m s^{-1}		$U_2 = 6.3 \times 10^{-4}$ m s^{-1}		$U_3 = 8.15 \times 10^{-4}$ m s^{-1}	
	B_o	ε	B_o	ε	B_o	ε
$h_1 = 3$ cm	4.43	0.625	3.78	0.661	3.71	0.705
$h_2 = 6$ cm	7.2	0.641	5.93	0.673	4.4	0.725
$h_3 = 9$ cm	9.5	0.678	7.31	0.708	6.24	0.742
$h_4 = 12$ cm	11.41		9.22	0.746	6.7	0.781
$h_5 = 15$ cm					10.87	
Different column zones	D_{axl} (m^2 s^{-1})	D_{axl} (m^2 s^{-1})	D_{axl} (m^2 s^{-1})			
$h_1 = 0$–3 cm	4.58×10^{-6}	7.575×10^{-6}	9.35×10^{-6}			
$h_2 = 3$–6 cm	3.44×10^{-6}	5.836×10^{-6}	8.41×10^{-6}			
$h_3 = 6$–9 cm	2.30×10^{-6}	4.13×10^{-6}	6.26×10^{-6}			
$h_4 = 9$–12 cm	1.77×10^{-6}	3.14×10^{-6}	5×10^{-6}			
$h_5 = 12$–15 cm			3.54×10^{-6}			

where C_{12} is the exit concentration that has left the 12-cm sample port and is measured at this port, $V_{f,12}$ is the volume of feed loaded onto the column until C_{12} reaches a certain degree of NPs breakthrough, $V_{L,0–12}$ is the liquid volume present in the bed voidage for the 0- to 12-cm column zone, and $V_{s,9–12}$ is the settled volume of adsorbent present in the 9- to 12-cm column zone.

Yield (%) is expressed as the amount of NPs adsorbed divided by the amount of NPs fed onto column [32].

Results and Discussion

Clean Feedstock Hydrodynamic Behavior

The results of the axial hydrodynamic research on clean feedstock within the modified NBG column are listed in Table 2 and provide evidence that non-uniform liquid behavior dominates this system. For a given stable condition, the mixing and dispersion actually vary along the bed height. The bottom regions of the bed experience severe mixing/dispersion, whereas these factors become less with increasing distance from the end of the bed. In addition, an increasing trend of voidage with the bed height at a certain degree of expansion and with the velocity at a certain bed position was observed. The inhomogeneous flow behavior in the bed is expected because of the following factors:

- Changes of bed voidage and mean particle diameter along the vertical axis (intensive interaction of particles in the bottom region lead to higher mixing/dispersion)
- Distributor effect becomes weaker with height above the distributor (Therefore, very calm channeling and a uniform velocity profile can be obtained in the top regions of the bed)
- Column diameter

NP Feedstock Hydrodynamic Behavior

As discussed before, the fluid nature plays a crucial role in the hydrodynamic properties and also effective adsorption performance within the EBA process. Although prior hydrodynamic studies were performed with the buffer alone in the modified NBG column, ultimately the hydrodynamic assessment of real nanobiological feedstock is also necessary in order to improve the prediction of adsorption behavior of nano/bioproducts before EBA operation.

Influence of Fluid Velocity on NP Hydrodynamic Behavior

Feed containing NPs with a constant concentration under different superficial velocities was fed into the column. Table 3 displays the effects of superficial flow velocity and bed height on the hydrodynamic behavior of the NPs. As expected, obvious variations of NP behavior occurred in the different bed regions. The Bodenstein number is lower in the zones near the distributor compared with those in the top zones of the bed. Also, an increasing trend of liquid back-mixing with increasing flow velocity at certain bed positions in the presence of NPs can be seen as similar to that observed in clean fluid (buffer). The fact is that severe convection and particle circulation can be caused by high flow velocity leading to greater mixing. Another result

Table 3 Axial mixing (B_o number) at various column heights under different conditions (NP feedstock)

Effect of flow velocity on NP hydrodynamics (C_o = 500 ppm)			
Different sampling positions	$U_1 = 4.2 \times 10^{-4}$ m s^{-1}	$U_2 = 6.3 \times 10^{-4}$ m s^{-1}	$U_3 = 8.15 \times 10^{-4}$ m s^{-1}
h_1 = 6 cm	8.12	6.3	5.68
h_2 = 9 cm	16.5	10.23	7
h_3 = 12 cm	26.83	15.73	10.77
h_4 = 15 cm			14.6

Effect of initial concentration on NP hydrodynamics ($U = 6.3 \times 10^{-4}$ m s^{-1})			
Different sampling positions	C_{o1} = 250 ppm	C_{o2} = 500 ppm	C_{o3} = 750 ppm
h_1 = 6 cm	7.89	6.3	6.2
h_2 = 9 cm	13.08	10.23	9.1
h_3 = 12 cm	20.5	15.73	14

obtained in the present study was that unclarified feedstock shows better behavior compared to clean feedstock within the modified NBG expanded bed column (Tables 2, 3). Adsorption of NPs to the adsorbent may be of benefit in achieving longer residence time and greater Bodenstein number than clean buffer hydrodynamics. Also improvement of liquid properties (density/viscosity) by addition of NPs to liquid may reduce mixing along the system.

Influence of Initial Concentration of Feed on NP Hydrodynamic Behavior

The solution of NPs with a constant velocity under different concentrations was introduced into the column. The effect of the initial concentration of NPs on the feed hydrodynamic behavior at different bed heights is presented in Table 3. Increasing the NP concentration promoted a pronounced decrease in Bodenstein number corresponding to increasing axial mixing within the EBA system. Nevertheless, aggregation and channeling are clearly additional phenomena which happen in the case of higher product concentration.

EA NP Adsorption Behavior within EBA System

BTCs were obtained at various column positions to evaluate NP adsorption behavior along the bed height. Moreover, adsorption particularity including DBC and yield based on BTCs were also calculated at different degrees of breakthrough to describe the axial adsorption kinetics exactly. The velocity of the mobile phase and target product initial concentration, in addition to bed height (position), play a critical role in BTCs development and adsorption properties in the EBA operation. This study delineated the individual contributions of these influential factors to NP breakthrough behavior.

NP Breakthrough Behavior Along the Bed Height

Figure 3a–e shows BTCs as a function of time at various axial positions of the bed under different conditions. Breakthrough data related to measured BTCs are summarized in Tables 4 and 5. As can be seen markedly from Fig. 3a–e, most of the NP BTCs have a sharp slope, indicating higher column efficiency in terms of NP capture. This trend reflects that NP DBCs do not vary very much with increasing level of breakthrough for steep curves. Diffusion resistance for NPs is very low due to the fact that NPs are very small biomolecules (they have small size or narrow size distribution). Therefore, these particles are able to penetrate the adsorbent easily which leads to a favorable adsorption equilibrium.

Another result was obtained here: as the front of the unbounded NPs moves up through the column, the shape of the BTCs becomes steeper along the bed height. In addition, the forms of the BTCs turn from a sharp slope to bulging and broad in the zone near the distributor (bed height of 6 cm). Results in Tables 4 and 5 suggest that under certain operation conditions, DBC and yield increase with distance from the end of the bed and these parameters are higher in the top bed zones than bottom regions at all degrees of breakthrough. Numerous reasons exist for the aforementioned trends including the following:

- There is some bypass flow in the bottom column zones, and liquid axial dispersion and back-mixing are relatively intensive in these regions. Larger circular movement of adsorbent in the bottom bed usually reflects poor stability of the system which causes reduction in DBC and NPs purification yield.
- Decreasing trend of liquid interstitial velocity with the bed height due to reduced bed voidage results in compressed shape of BTCs.

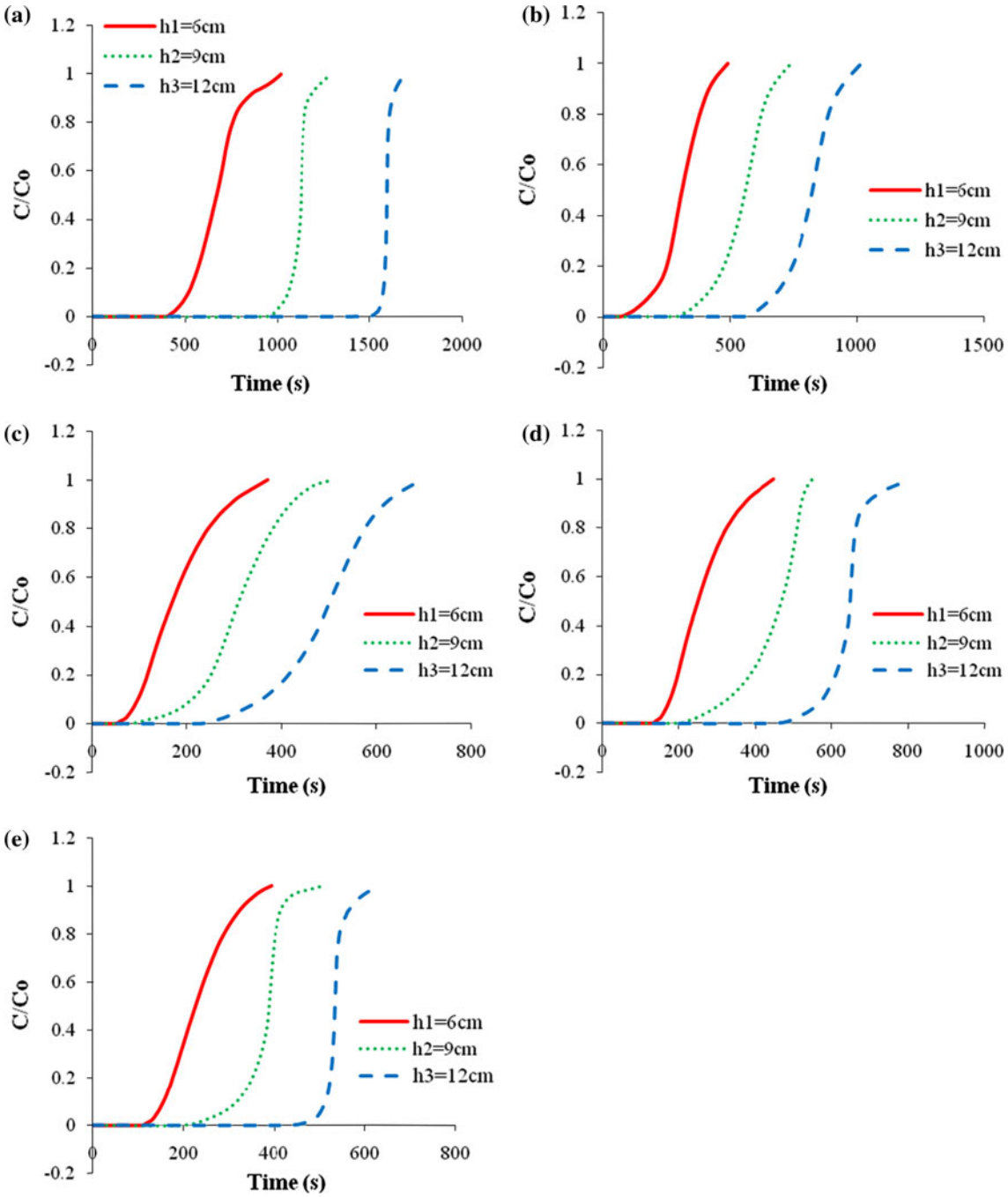

Fig. 3 EA NPs BTCs at various bed heights under different conditions: **a** $U_1 = 4.2 \times 10^{-4}$ m s^{-1}, $C_{o1} = 250$ ppm, **b** $U_2 = 6.3 \times 10^{-4}$ m s^{-1}, $C_{o1} = 250$ ppm, **c** $U_3 = 8.15 \times 10^{-4}$ m s^{-1}, $C_{o1} = 250$ ppm, **d** $U_2 = 6.3 \times 10^{-4}$ m s^{-1}, $C_{o2} = 500$ ppm, **e** $U_2 = 6.3 \times 10^{-4}$ m s^{-1}, $C_{o3} = 750$ ppm

- Classification of adsorbent particles was established in the EBA system. Smaller particles with a lower diffusional path length and larger specific surface in the top bed region improve mass transfer and, therefore, have higher capacity.

Influence of Fluid Velocity on NP Breakthrough

Figure 4a–c illustrates the effect of superficial liquid velocity on the NP BTCs at various bed heights. An apparent change in BTCs is observed in Fig. 4; reduction

Table 4 EA NP breakthrough data (DBC and yield) at various bed positions or zones under different liquid superficial velocities ($C_o = 250$ ppm)

Column zone (cm)	Breakthrough (%)	$U_3 = 8.15 \times 10^{-4}$ m s^{-1}		$U_2 = 6.3 \times 10^{-4}$ m s^{-1}		$U_1 = 4.2 \times 10^{-4}$ m s^{-1}	
		DBC (mg mL^{-1})	Yield (%)	DBC (mg mL^{-1})	Yield (%)	DBC (mg mL^{-1})	Yield (%)
0–6	0.2	2.23	82.2	1.40	70.0	0.75	51.3
	0.4	2.50	81.0	1.64	70.0	1.10	55.6
	0.6	2.61	78.4	1.79	67.0	1.30	54.4
	0.8	2.70	74.5	1.91	62.3	1.50	48.8
0–9	0.2	3.42	86.0	2.17	76.0	1.44	64.1
	0.4	3.51	85.5	2.44	75.2	1.70	65.2
	0.6	3.52	85.2	2.56	73.3	1.85	63.4
	0.8	3.53	84.56	2.64	70.41	2.0	58.3
0–12	0.2	4.10	87.1	3.05	79.3	2.27	69.4
	0.4	4.10	87.1	3.30	78.5	2.64	69.61
	0.6	4.10	87.0	3.40	77.2	2.81	68.1
	0.8	4.10	86.7	3.46	74.8	2.93	64.6
6–9	0.2	3.62		2.10		1.1	
	0.4	3.87		2.72		1.67	
	0.6	3.92		3.10		2.1	
	0.8	3.95		3.28		2.45	
9–12	0.2	4.75		2.8		1.7	
	0.4	4.82		3.7		3.04	
	0.6	4.83		4.0		3.6	
	0.8	4.86		4.28		4.03	

Table 5 EA NP breakthrough data (DBC and yield) at various bed positions or zones under different initial concentrations of NPs ($U = 6.3 \times 10^{-4}$ m s^{-1})

Column zone (cm)	Breakthrough (%)	$C_{o2} = 500$ ppm		$C_{o3} = 750$ ppm	
		DBC (mg mL^{-1})	Yield (%)	DBC (mg mL^{-1})	Yield (%)
0–6	0.2	2.05	65.0	2.61	61.2
	0.4	2.45	65.9	3.2	62.7
	0.6	2.75	63.6	3.6	61.0
	0.8	3.01	57.8	3.9	55.6
0–9	0.2	3.25	70.2	4.34	69.0
	0.4	3.8	70.1	4.75	69.0
	0.6	4.0	68.6	4.85	69.0
	0.8	4.1	67.0	4.91	67.2
0–12	0.2	4.74	75.2	5.9	72.3
	0.4	5.0	75.0	6.0	73.4
	0.6	5.03	74.6	6.01	72.1
	0.8	5.06	73.8	6.04	71.3
6–9	0.2	3.0		3.82	
	0.4	4.0		4.93	
	0.6	4.61		5.15	
	0.8	4.88		5.25	
9–12	0.2	4.5		6.06	
	0.4	5.4		6.39	
	0.6	5.6		6.51	
	0.8	5.7		6.6	

of the flow velocity can effectively increase the NP breakthrough time.

According to data reported in Table 4, it is clear that there was a drop in DBC and yield values when velocity increased. This means that at a certain point or zone of the bed, better adsorption performance of the NPs occurs in the lower flow velocity.

As discussed before, liquid velocity significantly affects the hydrodynamic and adsorption behavior within the EBA process. Increasing liquid dispersion with increasing

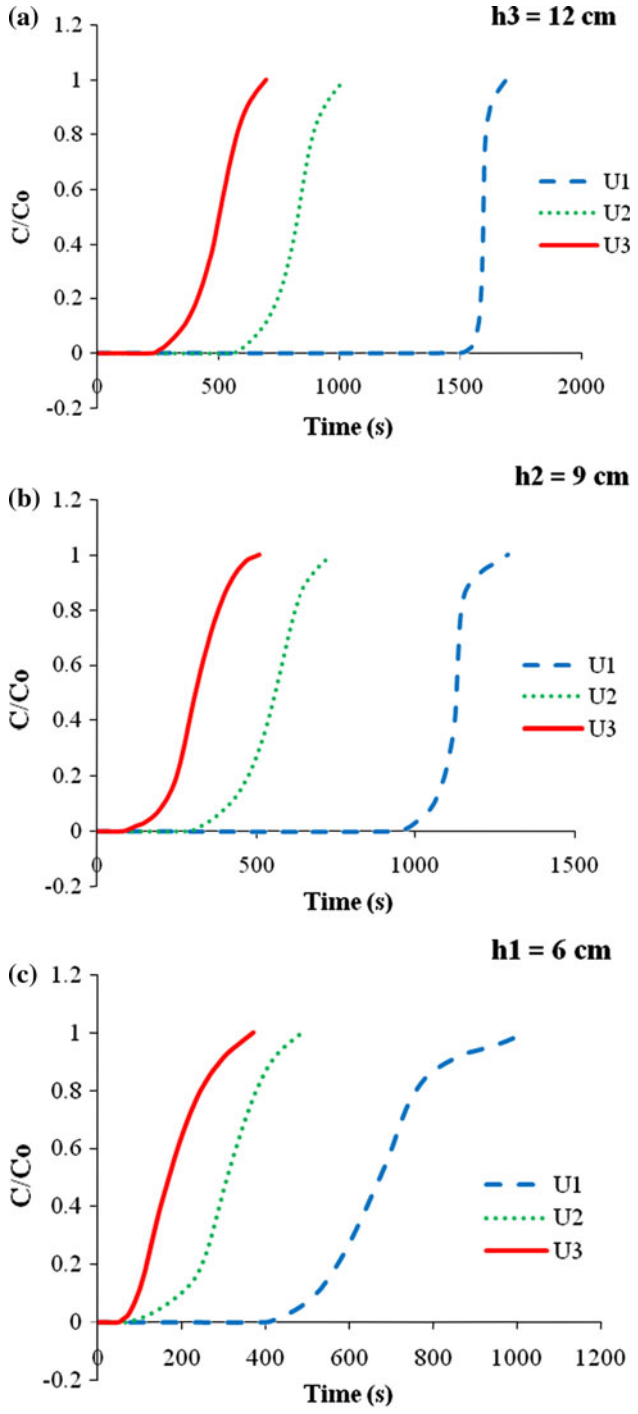

Fig. 4 Effect of superficial flow velocity on NP BTCs at different bed heights: $C_o = 250$ ppm, $U_1 = 4.2 \times 10^{-4}$ m s^{-1}, $U_2 = 6.3 \times 10^{-4}$ m s^{-1}, $U_3 = 8.15 \times 10^{-4}$ m s^{-1}

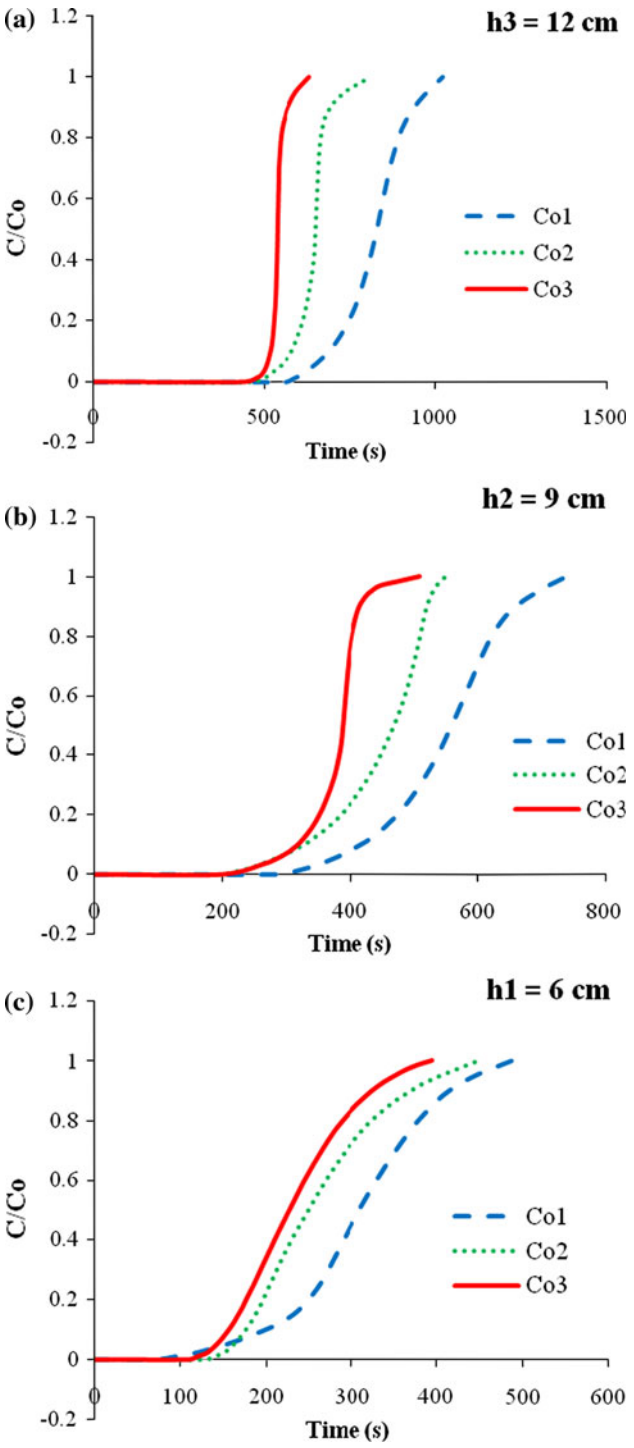

Fig. 5 Effect of initial concentration of NPs on BTCs at different bed heights: $U = 6.3 \times 10^{-4}$ m s^{-1}, $C_{o1} = 250$ ppm, $C_{o2} = 500$ ppm, $C_{o3} = 750$ ppm

velocity is one of the reasons for the reduction of adsorption performance.

Particle concentration is another contributing factor in the adsorption trend of nanobioproducts in the EBA system. Hence, an increasing trend of bed voidage with increasing velocity corresponding to decreasing adsorbent particles at each zone of the bed reduces the amount of adsorbed NPs.

Influence of Feed Initial Concentration on NP Breakthrough

The effect of the initial concentration of NPs on BTCs and adsorption particularity is shown in Fig. 5 and Table 5.

Figure 5 shows the product concentration in the sampling effluent takes a longer time to attain maximum breakthrough level when the load feed concentration is lower. Likewise, when the initial concentration of NPs in the feed increases, larger amounts of NPs bound in the adsorbent binding sites at the bed position or zone of interest (data presented in Table 5). This phenomenon is considered to be due to the higher NP concentration gradient between the liquid phase and adsorbent surface which results in larger NP mass flux.

Conclusions

The adsorption mechanism of nano/bioproducts is very complex in the EBA system and it is significantly affected by the NP hydrodynamic behavior through the column. The fabricated EA NPs were utilized herein not only mimic the size and surface chemistry of NPs such as viruses and plasmids, but also can be employed as a drug delivery system in their own right. Sampling of liquid phase in the presence of NPs and also RTD analysis were carried out at different positions of a modified simple customized NBG expanded bed contactor to evaluate the NP hydrodynamic exactly. The following results were obtained:

- The bottom regions of the bed experienced intensive liquid mixing/dispersion; as feed containing NPs progressed up the column, flow showed better behavior.
- Increasing key influential factors including the flow velocity and initial concentration of NPs led to increased mixing/dispersion in the EBA process.

Adsorption studies of NPs were performed at various points of the bed and the effect of the flow velocity and initial concentration of NPs on BTC formation, DBC, and purification yield was investigated along the bed height. Data obtained in this research confirmed the following:

- Steeper BTCs were achieved in the upper zones of the bed, and higher DBC and yield were also observed in these regions compared to bottom zones for all extents of breakthrough.
- Flow velocity had a significant negative influence on DBC and separation yield, whereas only DBC improved when the initial concentration of NPs increased.
- The best yield of the NP separation under the current conditions was 87 %, which is an excellent result for a one-pass expanded bed chromatography method.

The hydrodynamic properties of nano/bioproducts and their adsorption particularity at various bed points within a modified simple NBG column were discussed in detail for the first time in the present work. Hence, it is now possible to present a mathematical model for nano/bioproducts adsorption performance in the EBA process and this will be the subject of a future publication. EA NP adsorption is a simple and useful tool. Nevertheless, further research of other real NP biological feedstocks by this method should be performed.

Acknowledgments The authors would like to gratefully acknowledge members of the Nanotechnology Research Institute of Babol University of Technology, Babol, Iran.

References

1. Jahanshahi M, Ebrahimpour M (2009) Chromatographia 70:1553–1560. doi:10.1365/s10337-009-1369-4
2. Jahanshahi M, Najafpour Gh, Ebrahimpour M, Hajizadeh S, Shahavi MH (2009) Phys Status Solidi C 6(10):2199–2206. doi:10.1002/pssc.200881737
3. Jahanshahi M, Martinez L, Hajizadeh S (2008) J Chromatogr A 1203(1):13–20. doi:10.1016/j.chroma.2008.07.028
4. Padilha GdS, Curvelo-Santana JC, Alegre RM, Tambourgi EB (2009) J Chromatogr B 877:521–526. doi:10.1016/j.jchromb.2008.12.061
5. Pinotti LM, Fonseca LP, Prazeres DMF, Rodrigues DS, Nucci ER, Giordano RLC (2009) Biochem Eng J 44:111–118. doi:10.1016/j.bej.2008.11.006
6. Song H-B, Xiao Zh-F, Yuan Q-P (2009) J Chromatogr A 1216:5001–5010. doi:10.1016/j.chroma.2009.04.061
7. Zhao J, Lin D-Q, Wang Y-Ch, Yao Sh-J (2010) Carbohydr Polym 80:1085–1090. doi:10.1016/j.carbpol.2010.01.028
8. Li J, Chase HA (2009) J Chromatogr A 1216:8730–8740. doi:10.1016/j.chroma.2009.02.092
9. Vennapusa RR, Tari C, Cabrera R, Fernandez-Lahore M (2009) Biochem Eng J 43:16–26. doi:10.1016/j.bej.2008.08.004
10. Tong X-D, Sun Y (2002) J Chromatogr A 977:173–183. doi:10.1016/S0021-9673(02)01390-0
11. Yun J, Lin D-Q, Yao Sh-J (2005) J Chromatogr A 1095:16–26. doi:10.1016/j.chroma.2005.07.120
12. Li P, Xiu G, Rodrigues AE (2004) Chem Eng Sci 59:3837–3847. doi:10.1016/j.ces.2004.06.008
13. Moraes CC, Mazutti MA, Rodrigues MI, Filho FM, Kalil SJ (2009) J Chromatogr A 1216:4395–4401. doi:10.1016/j.chroma.2009.03.027

14. Balasundaram B, Harrison STL (2008) J Biotechnol 133:360–369. doi:10.1016/j.jbiotec.2007.07.724
15. Kaczmarski K, Bellot J-Ch (2005) J Chromatogr A 1069:91–97. doi:10.1016/j.chroma.2004.09.077
16. Yun J, Yao Sh-J, Lin D-Q (2005) Chem Eng J 109:123–131. doi:10.1016/j.cej.2005.03.015
17. Yun J, Yao Sh-J, Lin D-Q, Lu M-H, Zhao W-T (2004) Chem Eng Sci 59:449–457. doi:10.1016/j.ces.2003.10.009
18. Bruce LJ, Chase HA (2001) Chem Eng Sci 56:3149–3162 doi:10.1016/S0009-2509(00)00549-2
19. Willoughby NA, Hjorth R, Titchener-Hooker NJ (2000) Biotechnol Bioeng 69:648–653
20. Ebrahimpour M, Jahanshahi M, Hosenian AH (2010) Chromatographia 72:383–391. doi:10.1365/s10337-010-1676-9
21. Shahavi MH, Najafpour GD, Jahanshahi M (2008) Afr J Biotechnol 7(23):4336–4344
22. Rahimnejad M, Jahanshahi M, Najafpour GD (2006) Afr J Biotechnol 5(20):1918–1923
23. Mehravar R, Jahanshahi M, Saghatoleslami N (2009) Dyn Biochem Process Biotechnol Mol Biol 3:51–56
24. Mehravar R, Jahanshahi M, Saghatoleslami N (2009) Afr J Biotechnol 8(24):6822–6827
25. Jahanshahi M, Sanati MH, Hajizadeh S, Babaei Z (2008) Phys Status Solidi A 205:2898–2902. doi:10.1002/pssa.200824329
26. Jahanshahi M, Sanati MH, Babaei Z (2008) J Appl Stat 35:1345–1353. doi:10.1080/02664760802382426
27. Jahanshahi M, Sun Y, Santos E, Pacek A, Franco TT, Ninow A, Lyddiatt A (2002) Biotechnol Bioeng 80:201–212. doi:10.1002/bit.10360
28. Amersham Biosciences (1998) Expanded bed adsorption. Pharma Biotech, Uppsala
29. Jahanshai M, Pacek AW, Nienow AW, Lyddiatt A (2003) J Chem Technol Biotechnol 78:1111–1120. doi:10.1002/jctb.907
30. Biazus JPM, Severo J, Únior JB, Santana JCC, Souza RR, Tambourgi EB (2006) Process Biochem 41:1786–1791. doi:10.1016/j.procbio.2006.03.025
31. Najafpour GD (2007) Biochemical engineering and biotechnology, chap 17. Elsevier, Amsterdam
32. Ng MYT, Tan WS, Abdullah N, Ling TCh, Tey BT (2007) J Chromatogr A 1172:47–56. doi:10.1016/j.chroma.2007.09.065